Synthesis and Characterization of a Pt_3Ru_1/Vulcan Carbon Powder Nanocomposite and Reactivity as a Methanol Electrooxidation Catalyst

Joshua T. Moore,[†] James D. Corn,[†] Deryn Chu,[‡] Rongzhong Jiang,[‡] Deborah L. Boxall,[†] Edward A. Kenik,[§] and C. M. Lukehart[†,*]

Department of Chemistry, Vanderbilt University, Nashville, Tennessee 37235, Electrochemistry Branch, Sensors and Electron Devices Directorate, U.S. Army Research Laboratory, Adelphi, Maryland 20783-119, and the Metals and Ceramics Division, Oak Ridge National Laboratory, Oak Ridge, Tennessee 37831

Received January 10, 2003. Revised Manuscript Received April 21, 2003

Thermal treatment of $[Ru(2,3\text{-bis}(2\text{-pyridyl})quinoxaline)_3(PtCl_2)_3](BF_4)_2$/Vulcan carbon powder composites under reactive conditions forms Pt−Ru/carbon nanocomposites containing 27−34 wt % metal alloy as highly dispersed nanoparticles of ca. $Pt_{75}Ru_{25}$ stoichiometry. The metal nanoparticles have an average diameter of 6 nm (by TEM) and an fcc unit cell of lattice constant 3.907 (9) Å, as expected for Pt-rich Pt−Ru alloys. On-particle HR-EDS analysis indicates that gross phase separation of Pt and Ru does not occur on the nanoparticle scale. Evaluation of the performance of this nanocomposite as a methanol electrooxidation catalyst in a direct methanol fuel cell and in an electrochemical cell designed for combinatorial testing is reported.

Introduction

In direct-methanol fuel cells (DMFCs), aqueous methanol is electrooxidized to produce CO_2 and electrical current.[1] Electrocatalysts having higher activity for methanol oxidation are critically needed to achieve enhanced DMFC performance. The search for higher performing methanol oxidation catalysts has involved variation of both catalyst preparation strategy and catalyst composition.[1a]

Mixed-metal catalysts containing Pt are currently favored for methanol oxidation.[1] Pt activates the C−H bonds of methanol producing Pt−CO and other surface species, while an oxophilic metal activates water to accelerate oxidation of surface-adsorbed CO to CO_2. Although combinatorial studies indicate that ternary and quaternary alloy compositions can possess high activity as DMFC anode catalysts,[2] there remains much interest in improving the activity of more-established binary catalysts containing Pt and Ru.[1a] Unsupported Pt−Ru colloids and Pt−Ru/carbon nanocomposites have been prepared by a variety of chemical methods including solution-phase reduction of metal ions and thermal decomposition of either single-source or dual-source molecular precursors.[1,3] Carbonaceous support materials have included Vulcan carbon powder, carbon blacks, desulfurized carbon blacks, and fullerene soot.[3d] DMFC testing data indicate high performance when either unsupported or supported Pt−Ru catalysts are used, depending on anode catalyst composition and particle size.[3g,4]

A determination of the optimal Pt−Ru alloy composition for methanol electrooxidation remains elusive.[1a,5]

* To whom correspondence should be addressed. Phone: 615 322-2935. Fax: 615 322-4936. E-mail: charles.m.lukehart@vanderbilt.edu.
[†] Vanderbilt University.
[‡] U. S. Army Research Laboratory.
[§] Oak Ridge National Laboratory.

(1) (a) Hogarth, M. P.; Ralph, T. R. *Platinum Metals Rev.* **2002**, *46*, 146. (b) Ralph, T. R.; Hogarth, M. P. *Platinum Metals Rev.* **2002**, *46*, 117. (c) Hamnett, A. *Catal. Today* **1997**, *38*, 445. (d) Hogarth, M. P.; Hards, G. A. *Platinum Metals Rev.* **1996**, *40*, 150. (e) Chandler, G. K.; Genders, J. D.; Pletcher, D. *Platinum Metals Rev.* **1997**, *41*, 54. (f) Ralph, T. R. *Platinum Metals Rev.* **1997**, *41*, 102. (g) Hamnett A.; Troughton, G. L. *Chem. Ind.* **1992**, 480. (h) Ren, X.; Wilson, M. S.; Gottesfeld, S. *J. Electrochem. Soc.* **1996**, *143*, L12. (i) Hogarth, M. P.; Christensen, P. A.; Hammet, A. In *New Materials for Fuel Cell Systems I*; Proceedings of the 1st International Symposium on New Materials for Fuel Cell Systems, Montreal, July 9−13, 1995; p 310. (j) Lin, W. F.; Wang, J. T.; Savinell, R. F. *J. Electrochem. Soc.* **1997**, *144*, 1917. (k) Gasteiger, H. A.; Markovic, N.; Ross, P. N., Jr.; Cairns, E. J. *J. Electrochem. Soc.* **1994**, *141*, 1795. (l) Surampudi, S.; Narayanan, S. R.; Vamos, E.; Frank, H.; Halpert, G.; LaConti, A.; Kosek, J.; Surya Prakash, G. K.; Olah, G. A. *J. Power Sources* **1994**, *47*, 377. (m) Wang, K.; Gasteiger, H. A.; Markovic, N. M.; Ross, P. N., Jr. *Electrochim. Acta* **1996**, *41*, 2587. (n) Pathanjali, G. A.; Krishnamurthy, B.; Chireau, R. F.; Mital, C. K. *Bull. Electrochem.* **1996**, *12*, 193.

(2) (a) Reddington, E.; Sapienza, A.; Gurau, B.; Viswanathan, R.; Sarangapani, S.; Smotkin, E. S.; Mallouk, T. E. *Science* **1998**, *280*, 1735. (b) Gurau, B.; Viswanathan, R.; Liu, R.; Lafrenz, T.; Lye, K. L.; Smotkin, E. S.; Reddington, E.; Sapienza, A.; Chan, B. C.; Mallouk, T. E.; Sarabgapani, S. *J. Phys. Chem. B* **1998**, *102*, 9997. (c) Gotz, M.; Wendt, H. *Electrochim. Acta* **1998**, *43*, 3637.

(3) (a) Watanabe, M.; Uchida, M.; Motoo, S. *J. Electroanal. Chem.* **1987**, *229*, 395. (b) Nashner, M. S.; Frenkel, A. I.; Adler, D. L.; Shapley, J. R.; Nuzzo, R. G. *J. Am. Chem. Soc.* **1997**, *119*, 7760. (c) Nashner, M. S.; Frenkel, A. I.; Somerville, D.; Hills, C. W.; Shapley, J. R.; Nuzzo, R. G. *J. Am. Chem. Soc.* **1998**, *120*, 8093. (d) Hills, C. W.; Nashner, M. S.; Frenkel, A. I.; Shapley, J. R.; Nuzzo, R. G. *Langmuir* **1999**, *15*, 690. (e) Pan, C.; Dassenoy, F.; Casanove, M. J.; Philippot, K.; Amiens, C.; Lecante, P.; Mosset, A.; Chaudret, B. *J. Phys. Chem. B* **1999**, *103*, 10098. (f) Tess, M. E.; Hill, P. L.; Torraca, K. E.; Kerr, M. E.; Addoud, K. A.; McElwee-White, L. *Inorg. Chem.* **2000**, *39*, 3942. (g) Liu, L.; Pu, C.; Viswanathan, R.; Fan, Q.; Liu, R.; Smotkin, E. S. *Electrochim. Acta* **1998**, *43*, 3657. (h) Arico, A. S.; Creti, P.; Modica, E.; Monforte, G.; Baglio, V.; Antonucci, V. *Electrochim. Acta* **2000**, *45*, 4319.

(4) Arico, A. S.; Shukla, A. K.; El-Khatib, K. M.; Creti, P.; Antonucci, V. *J. Appl. Electrochem.* **1999**, 29, 671.

(5) (a) Lizcano-Valbuena, W. H.; Paganin, V. A.; Gonzalez, E. R. *Electrochim. Acta* **2002**, *47*, 3715. (b) Radmilovic, V.; Gasteiger, H. A.; Ross, P. N., Jr. *J. Catal.* **1995**, *154*, 98. (c) Gasteiger, H. A.; Markovic, N.; Ross, P. N., Jr.; Cairns, E. J. *J. Phys. Chem.* **1993**, *97*, 12020.

10.1021/cm030145f CCC: $25.00
Published on Web 07/11/2003

Smooth-metal Pt−Ru electrodes electrooxidize methanol most efficiently when the alloy composition is Pt rich. Carbon-supported Pt−Ru alloy catalysts appear to have surface alloy compositions strongly dependent on the method of synthesis and the thermal history of the sample. An optimal Pt−Ru alloy composition can be determined only by testing samples prepared using the same synthesis strategy.[1a] As an example, Gonzalez and co-workers report optimal DMFC performance for a $Pt_{75}Ru_{25}$/Vulcan carbon powder anode catalyst prepared by formic acid reduction of aqueous solutions of Pt and Ru chlorides.[5a] Hogarth and Ralph of Johnson Matthey have extensively studied the dependence of methanol electrooxidation activity on alloy particle composition for Pt−Ru/Vulcan carbon supported catalysts prepared using an aqueous-based slurry method.[1a] Electrochemical half-cell data indicate essentially constant, optimal activity for alloy compositions ranging from $Pt_{70}Ru_{30}$ to $Pt_{30}Ru_{70}$ with a composition of $Pt_{75}Ru_{25}$ expected to give slightly lower activity.

In a search for carbon-supported metal alloy DMFC anode catalysts that exhibit enhanced performance relative to that of commercial $Pt_{50}Ru_{50}$ unsupported catalysts, we have recently prepared Pt−Ru/carbon nanocomposites having an alloy composition of ca. $Pt_{50}Ru_{50}$ using the (1:1)-Pt,Ru dinuclear, single-source precursor complex, (η-C_2H_4)(Cl)Pt(μ-Cl)$_2$Ru(Cl)(η^3:η^3-2,7-dimethyloctadienediyl), as a source of metal.[6,7] When tested as an anode catalyst in a DMFC, the resulting cell performance of the $Pt_{50}Ru_{50}$/Vulcan carbon powder catalyst prepared by this method is essentially equivalent to that determined for a proprietary, unsupported $Pt_{50}Ru_{50}$ colloidal catalyst.

An interesting question arises as to the dependence of methanol oxidation performance on Pt−Ru particle stoichiometry for Pt−Ru/Vulcan carbon powder nanocomposites prepared by this single-source precursor method. On the basis of the results reported by Gonzalez and by Hogarth and Ralph, as summarized above, a supported catalyst having an alloy stoichiometry of ca. $Pt_{75}Ru_{25}$ prepared by this method might exhibit either slightly enhanced or slightly reduced performance relative to that of a $Pt_{50}Ru_{50}$ catalyst composition. Knowing that a $Pt_{50}Ru_{50}$/Vulcan carbon powder nanocomposite prepared by our single-source precursor protocol exhibits essentially the same DMFC performance as a commercial, unsupported $Pt_{50}Ru_{50}$ colloidal catalyst, the DMFC relative performance of a $Pt_{75}Ru_{25}$/Vulcan carbon nanocomposite prepared by this precursor method has been determined to address this question.

We now report the preparation of a Pt−Ru/Vulcan carbon powder nanocomposite having an alloy composition of ca. $Pt_{75}Ru_{25}$ using the tetranuclear, bimetallic, noncluster complex [Ru(2,3-bis(2-pyridyl)quinoxaline)$_3$-($PtCl_2$)$_3$](BF_4)$_2$ as a single-source precursor. To our knowledge, this is the first report of the preparation of a $Pt_{75}Ru_{25}$/Vulcan carbon powder nanocomposite using a single-source precursor synthesis strategy. The methanol electrooxidation performance of this nanocomposite and that of a commercial, unsupported $Pt_{50}Ru_{50}$ catalyst obtained from Johnson Matthey have been determined in a DMFC under identical conditions. Consistent with the trend reported by Hogarth and Ralph, the $Pt_{75}Ru_{25}$/Vulcan carbon nanocomposite prepared by this precursor method exhibits slightly reduced DMFC performance relative to that of the unsupported $Pt_{50}Ru_{50}$ catalyst. In addition, electrochemical measurements indicate that this supported catalyst has a slightly higher open-circuit-potential and higher current discharge at low current loads than does the commercial, unsupported $Pt_{50}Ru_{50}$ colloidal catalyst.

Experimental Section

Materials. The chemical reagents $NaBF_4$, 2,2′-pyridil, and 1,2-phenylenediamine were purchased from Aldrich Chemical Co. and were used as received. $RuCl_3$ was purchased from Strem Chemicals, Inc., and was used as received. Vulcan carbon powder XC-72R was purchased from Cabot Corporation. All solvents were reagent grade and used as received unless otherwise noted. *Cis*-$(DMSO)_2PtCl_2$[8] and 2,3-bis(2-pyridyl)quinoxaline (dpq)[9] were prepared according to literature procedures.

dpq =

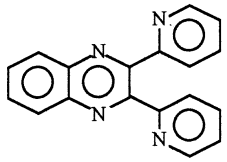

General Methods. Nanocomposite materials were characterized using a Philips CM20T transmission electron microscope (TEM) operating at 200 kV. Samples were prepared by dispersing a nanocomposite/CH_2Cl_2 suspension onto a 3-mm-diam copper grid covered with holey carbon film as a substrate and allowing the solvent to evaporate. Particle-size distributions were obtained by manually measuring particle diameters from bright-field TEM micrographs.

Single-particle high-spatial-resolution energy dispersive spectroscopy (HR-EDS) was used to examine variations in particle composition using a Philips CM200FEG 200 kV TEM equipped with an Oxford light element EDS detector and an EMiSPEC Vision data acquisition system at the SHaRE Collaboration Research Center in the Metals and Ceramics Division of Oak Ridge National Laboratory. The HR-EDS data were collected using a tilt angle of 15°, an acceleration voltage of 200 kV, a collection time of 20 s, and a 1.4-nm-diam probe in the stopped-scan mode. Integrated intensities from the Pt $L\alpha_1$ and the Ru $K\alpha_{1,2}$ lines were used for quantification because they were not overlapped by any other X-ray emissions. The X-ray emission cross sections appropriate for the instrumental geometry and the spurious contributions from the Vulcan carbon support were obtained by measuring Pt and Ru emission intensities for 100 s from several 1 μm^2 areas of a sample having a known bulk chemical composition. Ru emission intensities were corrected for any loss of Ru mass using a reported computational model.[6a]

Powder X-ray diffraction scans were obtained using a Scintag X_1 θ/θ automated powder diffractometer with a Cu target, a Peltier-cooled solid-state detector, and a zero-background, Si(510) sample support. For particle-size determinations, each XRD scan was corrected for background scattering and was stripped of the $K\alpha_2$ portion of the diffracted intensity using the DMSNT software (version 1.30c) provided by Scintag. Observed peaks were fitted with a profile function to extract the full-width-at-half-maximum (fwhm) values.

(6) (a) Boxall, D. L.; Deluga, G. A.; Kenik, E. A.; King, W. D.; Lukehart, C. M. *Chem. Mater.* **2001**, *13*, 891. (b) Lukehart, C. M. U.S. Patent 6,232,264, issued May 15, 2001.

(7) (a) Steigerwalt, E. S.; Deluga, G. A.; Cliffel, D. E.; Lukehart, C. M. *J. Phys. Chem. B* **2001**, *105*, 8097. (b) Steigerwalt, E. S.; Deluga, G. A.; Lukehart, C. M. *J. Phys. Chem. B* **2002**, *106*, 760.

(8) Price, J. H.; Williamson, A. N.; Schramm, R. F.; Wayland, B. B. *Inorg. Chem.* **1972**, *11*, 1280.

(9) Goodwin, H. A.; Lions, F. *J. Am. Chem. Soc.* **1959**, *81*, 6415.

Average crystallite size, L, was calculated from Scherrer's equation, $L = K\lambda/\beta\cos\theta_B$, assuming that peak broadening arises from size effects only (where β is the peak fwhm measured in radians on the 2θ scale, λ is the wavelength of X-rays used, θ_B is the Bragg angle for the measured hkl peak, and K is a constant equal to 0.90 for L taken as the volume-averaged crystallite dimension perpendicular to the hkl diffraction plane).[10] Chemical microanalyses were performed by Galbraith Laboratories, Knoxville, TN.

Preparation of Tris-[2,3-bis(2-pyridyl)quinoxaline]ruthenium(II) Tetrafluoroborate, $[Ru(dpq)_3](BF_4)_2$. The complex $[Ru(dpq)_3](BF_4)_2$ was synthesized using a variation of the method reported by Rillema, et al., for synthesis of the analogous PF_6^- salt.[11] To 50 mL of ethylene glycol were added 0.508 g (2.5 mmol) of $RuCl_3$ and 4.11 g (14.46 mmol) of dpq. The mixture was heated at reflux, under N_2, with constant stirring for 2 h. The solution was allowed to cool to room temperature, and then was filtered to remove unreacted dpq. Sufficient water was added to the filtrate to double the volume, and this solution was then added to a saturated solution of $NaBF_4$. The resulting precipitate was collected by vacuum filtration, dissolved in a minimum amount of CH_3CN, and developed on a neutral alumina column using CH_3CN as the eluent. The major red band was collected, and the solvent was then removed by rotary evaporation. The crude product was then redissolved in a minimum amount of CH_3CN and precipitated by addition of diethyl ether. The red powder precipitate was collected by vacuum filtration and dried at reduced pressure for 4 h (75% yield). Anal. Calcd for $C_{54}H_{36}N_{12}B_2F_8Ru\cdot 3H_2O$: C, 54.89; H, 3.58; N, 14.22. Found: C, 55.64; H, 3.38; N, 14.45.

Preparation of $[Ru(dpq)_3(PtCl_2)_3](BF_4)_2$, 1a. The tetranuclear complex $[Ru(dpq)_3(PtCl_2)_3](BF_4)_2$ was synthesized according to a variation of the method reported by Rillema and Sahai for synthesis of the analogous PF_6^- salt.[12] A 0.301-g portion (0.267 mmol) of $[Ru(dpq)_3](BF_4)_2$ and 0.470 g (1.11 mmol) of *cis*-$(DMSO)_2PtCl_2$ were dissolved in 100 mL of deoxygenated methanol. The solution was heated at reflux, under N_2, in the dark for 12 h. The resulting purple suspension was cooled to −30 °C for 6 h, then filtered, and the collected solid was washed with cold methanol. The product was dried at reduced pressure for 16 h (70% yield). As observed in the synthesis of the analogous PF_6^- salt,[12] elemental analysis data confirmed retention of 3 equivalents of water of crystallization in the final product. Anal. Calcd for $C_{54}H_{36}N_{12}B_2Cl_6F_8RuPt_3\cdot 3H_2O$: C, 32.76; H, 2.14; N, 8.49. Found: C, 32.43, H, 2.40; N, 8.00.

A UV−Visible absorption spectrum of an acetonitrile solution of complex **1a** was essentially identical to that reported for the analogous PF_6^- complex[12] and revealed only a negligible concentration of unreacted cis-$(DMSO)_2PtCl_2$ (see Supporting Information).

Preparation of a $Pt_{75}Ru_{25}$/Vulcan Carbon Nanocomposite, 1b. A Pt−Ru/Vulcan carbon powder nanocomposite was prepared using a four-cycle deposition/thermal treatment process. Approximately equal masses (42 mg) of $[Ru(dpq)_3(PtCl_2)_3](BF_4)_2$, **1a**, were dissolved in 30 mL of CH_2Cl_2 and slurried with 90 mg of Vulcan carbon powder. The solvent was then removed at reduced pressure to complete adsorption of the complex onto the carbon support. After each of the four deposition cycles, the composite material was oxidized in a tube furnace by heating the sample to 300 °C at a rate of 15 °C/min in a flow (150 mL/min) of dry air followed by immediate cooling in a stream of dry N_2. Following the final deposition, the resulting material was heated to 650 °C at a rate of 15 °C/min in a flow of 10% H_2/90% N_2, commonly called "getter gas", and the sample was held at this temperature for 1 h. The sample was then cooled to room temperature under N_2. Anal. found: Pt, 23.41; Ru, 4.11; ($Pt_{2.95}Ru_1$).

A Pt−Ru/Vulcan carbon powder nanocomposite, **1c**, was also prepared using a 3-cycle adsorption/thermal treatment protocol and only reducing or inert gaseous atmospheres. A total of 1.10 g of precursor complex **1a** were absorbed onto 0.390 g of Vulcan carbon powder. After each deposition, the sample was placed in a combustion boat, heated to 350 °C at a ramp rate of 15° C per minute under a getter gas atmosphere, and cooled with a N_2 purge (approximate cooling rate of 2.4 °C per minute). Following the third and final heat treatment, the sample was annealed under a nitrogen atmosphere at 350 °C for 30 min and then cooled to room temperature. The final mass of the nanocomposite **1c** of 934 mg is consistent with retention of ca. 160 mg of nonmetallic mass from precursor decomposition. Anal. found: C, 53.70; H, 0.98; N, 4.34; Pt, 29.79; Ru, 4.82; ($Pt_{3.21}Ru_1$). Although Pt−Ru/carbon nanocomposites prepared under either reducing or oxidizing-then-reducing conditions are essentially identical by TEM or XRD, the latter (**1b**) performed better as methanol electrooxidation catalysts.

Direct Methanol Fuel Cell and Electrochemical Testing Procedures. Nanocomposite **1b** and a commercial unsupported $Pt_{50}Ru_{50}$ colloid (Johnson Matthey HiSPEC 6000) were comparatively tested as methanol electrooxidation catalysts using combinatorial electrochemical measurements and working DMFC test fixtures. Combinatorial electrochemical measurements were performed using proprietary technology developed at the Army Research Laboratory.[13] Anode electrodes were spotted on a graphite plane with an exposed surface area of 0.03 cm^2 for each sample tested and a sample loading of 0.2 mg. The cathode was Pt black (Johnson Matthey HiSPEC 1000, 27 m^2/g) having a larger exposed surface area. An electrolyte probe consisting of 3 M H_2SO_4 was used to connect anode and cathode electrodes and form separated methanol fuel cells. The anode fuel was 3 M methanol in 3 M H_2SO_4 under an Ar atmosphere, while the cathode fuel was air. All measurements were recorded at 20 °C. For DMFC testing, membrane electrode assemblies were fabricated using either nanocomposite **1b** or the commercial Pt_1Ru_1 colloid as the anode catalyst with a loading of 1 mg/cm^2 total metal. The cathode catalyst was Pt black (Johnson Matthey) at a loading of 3 mg/cm^2. Membrane material was Nafion 117. The anode fuel was 1 M methanol at a flow rate of 2.5 mL/min. The cathode fuel was air at a flow rate of 600 sccm at 0 psi gauge pressure.

Results and Discussion

Adsorption of the (3:1)-Pt,Ru tetranuclear, bimetallic precursor complex **1a** from solution phase onto Vulcan carbon powder followed by removal of residual solvent at reduced pressure affords a precursor **1a**/carbon composite as a dry, black powder (see eq 1). Thermal treatment under oxidizing-then-reducing gaseous atmospheres reactively degrades the precursor complex and forms a Pt−Ru/Vulcan carbon powder nanocomposite material, **1b**. Although the identity of evolved degradation products has not been determined experimentally, the observed mass loss during thermal treatment is consistent with essentially complete loss of the nonmetallic elements present in precursor **1a**. Nanocomposite **1b** has been prepared with 27−34 wt % total metal loading depending on the relative mass of carbon powder and precursor **1a** used in the synthesis. A multistep protocol for precursor deposition/degradation ensures high dispersion of metal nanoparticles on the carbon support. Thermal degradation of precursor

(10) Klug, H. P.; Alexander, L. E. *X-ray Diffraction Procedures for Polycrystalline and Amorphous Materials*, 2nd ed.; Wiley: New York, 1974.

(11) Rillema, D. P.; Taghdiri, D. G.; Jones, D. S.; Keller, C. D.; Worl, L. A.; Meyer, T. J.; Levy, H. A. *Inorg. Chem.* **1987**, *26*, 578.

(12) Rillema, D. P.; Sahai, R. *J. Chem. Soc., Chem. Commun.* **1986**, 1133.

(13) (a) Jiang, R.; Chu, D. *J. Electroanal. Chem.* **2002**, *527*, 137. (b) Patent pending.

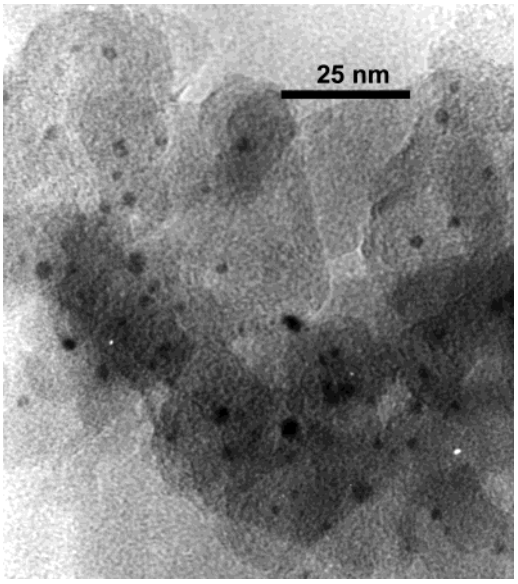

Figure 1. Bright-field TEM micrograph of nanocomposite **1b**.

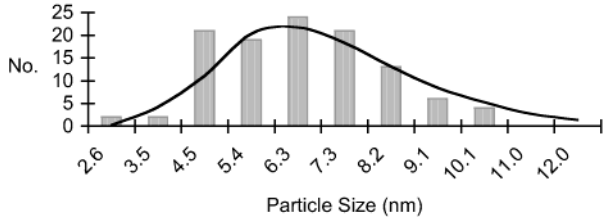

Figure 2. Histogram of metal nanoparticle diameters as measured from TEM micrographs for nanocomposite **1b** showing a superimposed calculated log-normal distribution curve.

1a/Vulcan carbon composites under solely reducing conditions affords nanocomposites (**1c**) essentially identical to **1b**; however, significant retention of nonmetallic precursor mass is observed under these synthesis conditions.

$$[Ru(dpq)_3(PtCl_2)_3](BF_4)_2,\ \mathbf{1a} + \text{C powder} \xrightarrow{\text{soln adsorption/deposition}} \text{precursor } \mathbf{1a}/\text{C composite} \xrightarrow{\Delta,\ \text{air, } N_2 \text{ or } (1{:}9)\ H_2{:}N_2} \text{nano-Pt-Ru/Vulcan carbon } \mathbf{1b\text{-}c} \quad (1)$$

A representative bright-field TEM micrograph of nanocomposite **1b** is shown in Figure 1. Metal particles of high contrast are observed widely dispersed over the Vulcan carbon powder support. A histogram of metal particle diameters (Figure 2) reveals metal particle sizes ranging from 3 to 10 nm with an average diameter of 6.0 nm. The observed log-normal particle-size distribution is consistent with a coalescence growth mechanism for surface-supported metal particles.[14]

A broad-area EDS spectrum of nanocomposite **1b** is shown in Figure 3. The expected emission lines from Pt and Ru are evident along with emission from the copper grid of the sample holder and very weak silicon emission due to trace amounts of clay present within the carbon powder support. The relative integrated intensity of appropriate pairs of Pt and Ru emission lines gives a calculated Pt/Ru atomic ratio of 3:1 on the micron scale. Chemical elemental analysis of nanocomposite **1b** gives a Pt/Ru atomic ratio of $Pt_{2.95}Ru_1$ that is consistent, within experimental error, with both the metal stoichiometry of precursor **1a** and the Pt/Ru stoichiometry determined by broad-area EDS. Previous study of repetitive chemical elemental analysis of identical samples of Pt−Ru/carbon nanocomposites gives an experimental precision of ±0.08 on Pt/Ru atomic ratios determined from commercial elemental analytical data.[5a]

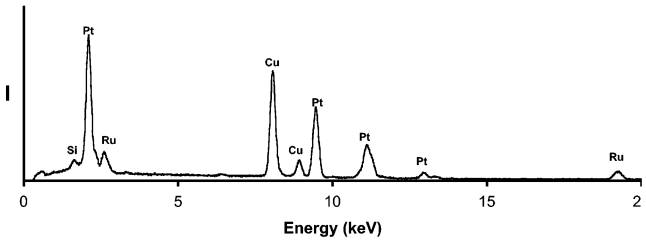

Figure 3. EDS spectrum of nanocomposite **1b** showing the expected Pt and Ru emission lines, Cu emission from the copper grid contained in the sample holder, and weak Si emission from a trace amount of silicate clay present in the Vulcan carbon support.

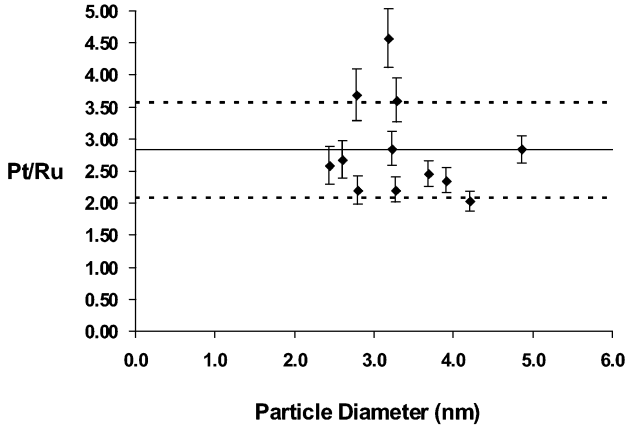

Figure 4. Plot of Pt:Ru atomic ratios measured by HR-EDS for individual metal alloy nanoparticles within nanocomposite **1b**.

To investigate the compositional integrity of individual nanocrystals prepared using this synthesis strategy, the Pt/Ru atomic ratio of twelve randomly chosen nanocrystals within nanocomposite **1b** have been measured experimentally by HR-EDS. The integrated intensities of the Pt $L\alpha_1$ and Ru $K\alpha_{1,2}$ emissions from *individual* alloy nanoclusters were collected using a field-emission gun with a spot size of 1.4 nm and were converted into Pt/Ru atomic ratios as previously described.[5a] A plot of Pt/Ru atomic ratios versus nanocluster size for nanocrystals within nanocomposite **1b** is shown in Figure 4. Error bars for the Pt/Ru atomic ratios are calculated from error propagation and are based principally on EDS counting statistics.

As to compositional variation on the nanocluster scale, only statistical arguments can be made. HR-EDS measurements indicate the absence of detectable amounts of Pt or Ru in regions of the carbon support not containing nanoparticles, so the metal content of these

(14) Granqvist, C. G.; Buhrman, R. A. *J. Catal.* **1976**, *42*, 477.

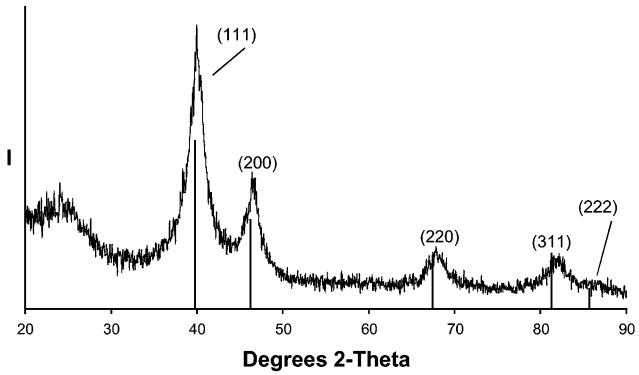

Figure 5. Powder XRD scan of nanocomposite **1b** recorded with Cu Kα radiation along with the line pattern of bulk Pt metal.

samples appears to be localized primarily within observable nanoparticles. The average Pt/Ru stoichiometry for nanoclusters within nanocomposite **1b** is 2.84 ± 0.75, where the standard deviation is weighted for the experimental uncertainty associated with each on-particle measurement. This error is principally due to experimental uncertainties associated with the HR-EDS counting statistics, but also could include particle-to-particle variation in metal stoichiometry. On-particle Pt/Ru average stoichiometry is within one standard deviation of Pt/Ru stoichiometry determined by bulk chemical elemental microanalysis and that expected from the 3:1 Pt/Ru stoichiometry of precursor **1a**. Although individual particle Pt/Ru atomic ratios range from ca. 2.0−4.5 with relatively low precision, gross phase separation of the two metals within nanocomposite **1b** is not evident on the nanoscale among the particles examined.

A powder XRD scan of nanocomposite **1b** is shown in Figure 5. Amorphous scattering from the carbon powder support is evident by the broad peak near 24° in 2θ. All of the remaining predominant peaks are consistent with the face-centered-cubic (fcc) pattern expected for Pt-rich Pt−Ru alloys. Peaks associated with this alloy phase are identified by the appropriate Miller indices. The cell constant calculated from XRD peak positions is 3.907 (9) Å.[7a] Gonzalez and co-workers report a cell constant of 3.9107 Å for Pt−Ru alloy particles of composition $Pt_{75}Ru_{25}$ (though a standard deviation value was not given).[5a] Scherrer's analysis of experimentally measured XRD peak widths for nanocomposite **1b** gives a calculated average crystalline domain size of 3.2 nm for the alloy nanoparticles.[10] Diffraction peaks near 38° and 44° in 2θ from Ru metal are not observed, so any crystalline metal phase separation that might have occurred during synthesis is not evident.

The reactivity of nanocomposite **1b** as a methanol electrooxidation catalyst relative to that of a commercial unsupported $Pt_{50}Ru_{50}$ colloid has been evaluated using both a combinatorial electrode test fixture and a working DMFC. The discharge performance curves shown in Figure 6 provide a direct comparison of these two electrocatalysts in a combinatorial fuel cell test fixture at identical metal loading. While nanocomposite **1b** gives a slightly higher open-circuit potential and higher performance at lower current densities, the unsupported $Pt_{50}Ru_{50}$ catalyst outperforms nanocomposite **1b** at current loads greater than ca. 0.25 mA. A lower relative

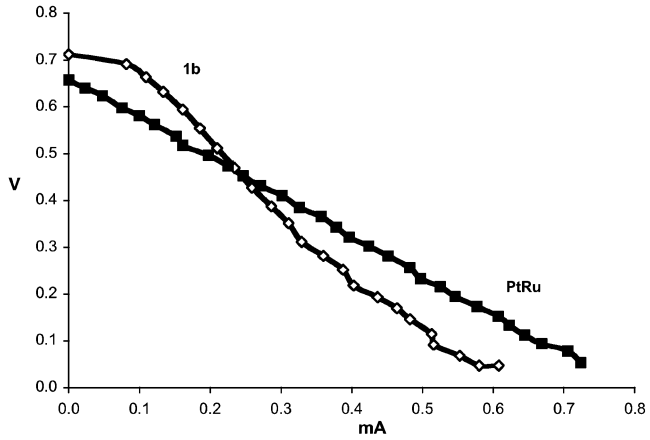

Figure 6. Plots of the discharge curves of nanocomposite **1b** and a commercial (1:1) Pt−Ru colloid obtained from Johnson Matthey (PtRu) as methanol electrooxidation catalysts in a combinatorial electrochemical test fixture.

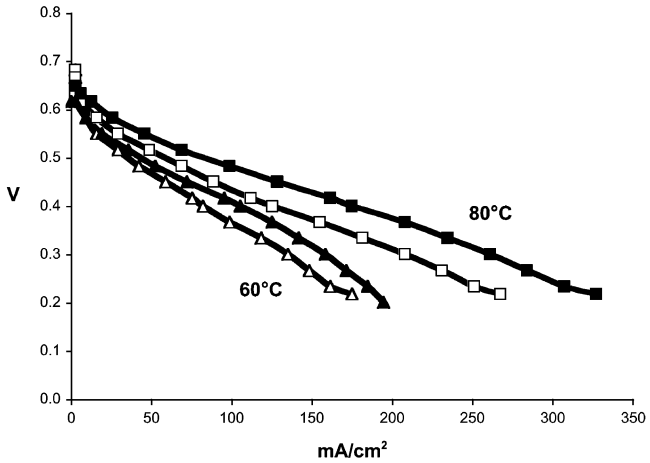

Figure 7. Plots of the relative cell performance of nanocomposite **1b** (open triangles or squares) and a commercial $Pt_{50}Ru_{50}$ colloid (filled triangles or squares) obtained from Johnson Matthey (JM) as methanol electrooxidation catalysts in a DMFC test fixture. Anode catalyst loadings are identical at 1 mg total metal/cm^2. Performance curves were measured at operating temperatures of 60 °C (open or filled triangles) and 80 °C (open or filled squares).

performance for a supported catalyst relative to that of an unsupported catalyst at higher current loading is a common observation. To obtain the same metal loading, a thicker reaction layer is required for supported catalysts, thereby reducing reactant diffusion and proton transport rates at high currents. These inefficiencies reduce relative catalyst performance for supported catalysts, such as nanocomposite **1b**, at higher current loads.

Performance curves for DMFCs having either nanocomposite **1b** or the same commercial, unsupported $Pt_{50}Ru_{50}$ colloid as anode catalyst are shown in Figure 7 for cells operating at 60 °C and 80 °C. Anode catalyst loadings are identical at 1 mg total metal/cm^2. As expected, cell performance drops significantly with decreasing temperature, and no unusual temperature dependence is observed for either catalyst.[1a] At each temperature, the pair of catalysts exhibit essentially parallel relative performance, with the unsupported catalyst performing slightly higher than nanocomposite **1b** at the same current density. These performance curves indicate that while nanocomposite **1b** performs

well as a methanol electrooxidation catalyst, it does not exhibit exceptional performance relative to that of a commercial unsupported $Pt_{50}Ru_{50}$ colloid catalyst. Comparison of the relative DMFC performance of nanocomposite **1b** to that of a $Pt_{50}Ru_{50}$/Vulcan carbon nanocomposite prepared by the same synthesis strategy[6a] reveals that increasing the Pt content of the Pt−Ru alloy particles from ca. $Pt_{50}Ru_{50}$ to ca. $Pt_{75}Ru_{25}$ leads to a slight reduction in DMFC performance. There appears to be no advantage in using Pt-rich precursors of complex composition. Better performance is achieved by using a (1:1)-Pt,Ru precursor of simpler construction. The atomic ratio of $Pt_{50}Ru_{50}$ is generally observed to be the most practical anode catalyst for DMFCs.[1]

Acknowledgment. Research support provided by the U.S. Army Research Office under grants DAAH04-95-1-0146, DAAH04-96-1-0179, DAAH04-96-1-0302, and DAAG55-98-1-0362 is gratefully acknowledged by C.M.L. On-particle EDS and HR-TEM measurements performed at the Oak Ridge National Laboratory SHaRE Collaborative Research Center were sponsored by the Division of Materials Sciences and Engineering, U.S. Department of Energy, under contract DE-AC05-00OR22725 with UT-Battelle, LLC. D.C and R.J. acknowledge support received through the U.S. Army Research Laboratory Director's Research Initiative Program. We thank Mr. J. A. Michel, Mr. J. M. Slocik, and Dr. D. W. Wright for their assistance.

Supporting Information Available: Sketch of the structural formula of the cation of complex **1a** and UV−Visible absorption spectra of solutions of complex **1a** and of cis-$(DMSO)_2PtCl_2$ in acetonitrile. This material is available free of charge via the Internet at http://pubs.acs.org.

CM030145F